

Spudcan-pile interaction during installation of piles for offshore wind turbines

P. Staubach*

M. Lücke

Bauhaus-Universität Weimar, Weimar, Germany

S. Raymackers

DEME Group, Belgium

B. Bienen

Centre for Offshore Foundation Systems, The University of Western Australia, Australia

*patrick.staubach@uni-weimar.de (corresponding author)

ABSTRACT: This work investigates the effects of the pile installation process on spudcans used as temporary foundations, employing numerical analysis to incorporate large deformations, dynamic wave propagation, and hydro-mechanical coupling for the first time. A hydro-mechanically coupled Coupled Eulerian-Lagrangian (CEL) method is employed to meet these requirements. The simulations aim to replicate the full process of spudcan penetration in the seabed, followed by the pile driving process. This is realised in a fully explicit time integration scheme, for which a method is outlined to achieve a static equilibrium of the spudcan prior to the start of the pile driving process. The results reveal that with decreasing distance between the pile and spudcan, the spudcan is influenced by the pile installation process, leading to additional settlements.

Keywords: spudcan installation; pile installation; spudcan-pile interaction; large deformations; hypoplasticity

1 INTRODUCTION

Jack-up vessels are often used for installation of foundations of offshore wind turbines. A jack-up will pre-drive its legs, fitted with spudcans, before going to working height. The objective of the pre-driving is to penetrate the spudcans under controlled conditions, in or near the water, to a depth at which the soil has sufficient bearing capacity to have no additional penetration during the operations to follow. With the larger jack-ups which can install monopiles, the distance between the monopile and the spudcans is given by the location of the gripper on the vessel. Jacket piles can be installed from a jack-up with a template hanging under the vessel hull, attached to the legs. After jacking the template will be lowered to the seabed and piles will be installed by impact hammering. It is noted that in some cases the spudcans may be affected by the impact hammering of the piles. Particularly in case of loosely bedded sandy soils large excess pore water pressure can build up around the spudcan due to their tendency to contract.

Guidelines on critical distances typically emphasise the impact of spudcan proximity on pile foundations rather than the installation-induced effects on the spudcan itself. The American Bureau of Shipping (ABS) suggests for certain ground conditions that when the proximity of a spudcan to a pile is less than one spudcan diameter (edge-to-edge), a

comprehensive assessment should be undertaken to estimate the severity of any interaction problems. If the proximity of the spudcan to the pile is less than this distance, detailed analysis is recommended to assess the severity of any spudcan-pile interaction issues that may arise during the installation process.

The SNAME J-REG JIP guidelines specifically address pile installation-induced interactions and their effects on spudcan behavior. Consistent with ABS recommendations, numerical analyses are suggested in scenarios where pile driving could lead to a loss of soil strength beneath the spudcan. These detailed assessments often require the use of advanced numerical models to accurately capture the complex interactions involved.

The numerical investigation of processes occurring during offshore pile installation is a challenging task: large deformations occur during pile installation, excess pore water pressures are generated, which partially dissipate due to consolidation during driving, and inertia effects due to impact driving need to be considered. To date, in most analyses either the penetration behaviour of jack-up spudcans (see e.g. Wu et al., 2019) or the pile installation process (see e.g. Staubach et al., 2022) have been investigated, but only a limited number of sophisticated numerical analyses of the combined process exist. Recent centrifuge tests highlight the relevance of these

interaction effects for practical considerations (Falcon et al., 2023). Chow et al. (2021) and Tho et al. (2013) present simplified numerical analyses of the spudcan-pile interaction, but without considering dynamic effects utilising constitutive models able to consider strain-dependent stiffness.

In this paper, a numerical framework is presented that considers large deformations, dynamic wave propagation and hydro-mechanical coupling allowing to identify critical settings for the spudcan-pile interaction during the installation of piles for offshore wind turbines. The focus of this investigation is the pile installation induced effect on the spudcan, rather than potential spudcan induced effects on piles.

2 NUMERICAL MODEL

The study investigates pile installation near spudcans, focusing on the impact of pile proximity on spudcan stability. The problem position is depicted in Figure 1. The distance between the spudcan and pile is defined by the parameter a . Two configurations are modeled: a monopile with a diameter of $D_m = 6.5$ m and a distance of $a_m = 21$ m from the spudcan, and a jacket-pile with a diameter of $D_j = 3.5$ m and distance $a_j = 4.45$ m. The pile thicknesses are $t_m = 0.07$ m and $t_j = 0.045$ m. The model and the dimensions of the spudcan are given in Figure 2. With a diameter of the spudcan of $D_s = 12.4$ m, the normalized distances for the monopile and jacket-pile are $\frac{a_m}{D_s} = 1.69$ and $\frac{a_j}{D_s} = 0.36$, respectively.

Two soil layers having the same mechanical properties but different relative density are considered as shown in Figure 1: the upper layer of 8 m thickness has a relative density of 50%, while the lower layer is very dense with a relative density of 100 %. This ground condition is considered to be a critical yet realistic scenario. The simulations are performed using the Coupled Eulerian-Lagrangian (CEL) method implemented in Abaqus (see e.g. Wang et al., 2015), where the pile and spudcan are modeled within the Lagrangian framework, while the soil is modelled within the Eulerian framework. This approach allows for the simulation of large deformations occurring at both the spudcan-soil interface and the pile-soil interface. The interface conditions are identical for both spudcan and pile, considering rough surfaces with an interface friction angle of 30° . Both spudcan and pile are modelled as rigid bodies, assuming that they

show negligible intrinsic deformations. Note that both the pile penetration and the spudcan penetration processes start from the soil surface. In order to avoid large influence from reflected waves at the model boundary, a large soil volume with a depth of 100 m and 75 m in x- and y-direction is considered.

Karlsruhe Fine Sand (KFS) is considered as sand. KFS is a fine sand with a hydraulic conductivity of $k^w = 4 \cdot 10^{-5}$ m/s. The hypoplastic model (version of von Wolffersdorff, 1996) with intergranular strain (Niemunis et al., 1997) is used as constitutive model, which allows to account for most mechanical aspects relevant to the boundary value problem at hand. The parameters have been calibrated using monotonic and cyclic test data and are provided in Table 1.

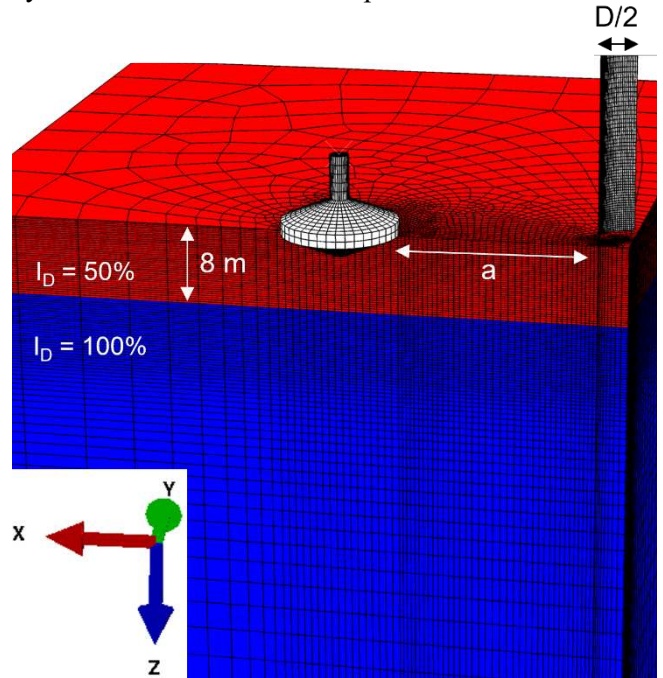


Figure 1. Numerical model adopted for the analyses. The distance between pile and spudcan a is given. In addition, the relative densities of the two sand layers are given.

Hydro-mechanically coupled analyses are performed to account for the buildup of excess pore pressure while simultaneously considering consolidation effects. For this purpose, the approach outlined in Hamann et al. (2015) and Staubach et al. (2020), Staubach (2024) is adopted. Effects resulting from possible cavitation during the driving process are considered according to Staubach et al. (2023), assuming a water depth of 20 m. All subroutines utilised in this work are available from the github account of the first author: <https://github.com/patrickstaubach>.

Table 1. Parameters of the hypoplastic model with intergranular strain for KFS (see Wichtmann, 2016)

φ_c	h_s	n	e_{do}	e_{co}	e_{io}	α	β	m_T	m_R	R	β_R	χ
[°]	[kPa]	[-]	[-]	[-]	[-]	[-]	[-]	[-]	[-]	[-]	[-]	[-]
33.12	$4 \cdot 10^6$	0.27	0.677	1.054	1.212	0.14	2.5	1.2	2.4	0.0001	0.1	6

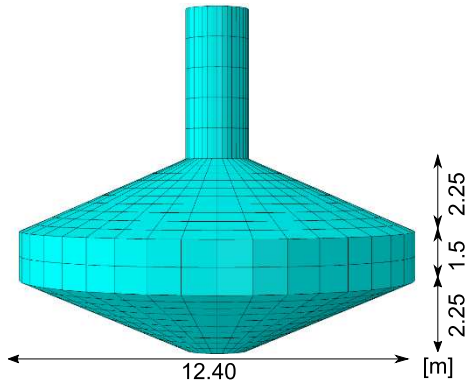


Figure 2. Model of the spudcan with dimensions

Boundary conditions are set to allow realistic movement: the spudcan is free to move in the x and z directions (see Figure 1 for the coordinate system), while the pile is restricted to movement in the z direction. Soil movement is restricted to move along the symmetry axes, with drainage allowed at the seabed to capture pore pressure evolution.

2.1 Load sequence on the spudcan and pile

Since the CEL method is only implemented with explicit time integration, all simulation steps must be performed dynamically considering acceleration and inertia effects. This poses challenges for the current analysis, as the penetration of the spudcan into the soil, as well as the self-weight penetration of the pile, are processes that occur over extended physical timescales. In this simulation, the goal is to consider both processes in sequence: first, the penetration of the spudcan into the soil, followed by the pile installation process.

Numerically, there is currently no method to model both processes while maintaining real physical time, as explicit time integration schemes are restricted to small time increments. Therefore, in the present simulations, the processes of spudcan penetration and the self-weight penetration of the pile are accelerated. To ensure that despite this acceleration nearly quasi-static conditions are maintained, i.e. the spudcan is in static equilibrium once the operational load is acting, viscous pressure loads are used. Viscous pressure loads can be utilised to suppress low-frequency dynamic effects, ensuring a faster convergence to static equilibrium with minimal computational increments. These loads act as distributed pressures and are considered on the spudcan surface in contact with the soil. The viscous pressure is calculated based on the velocity of the spudcan and a viscosity coefficient. The larger the viscosity coefficient is, the larger the absorbed energy and the faster a static equilibrium is achieved. For the simulations, the

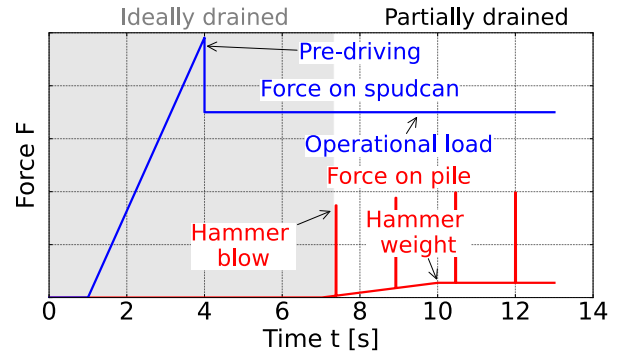


Figure 3. Applied forces to the pile (excluding self-weight) and the spudcan

viscosity coefficient was calculated as 10 % of the dilatational soil wave velocity times its density.

The load sequence applied to the spudcan reflects realistic operational conditions and is shown in Figure 3. An initial pre-driving load is applied, followed by a steady operational load. This analysis is performed under fully drained conditions, meaning that no excess pore water pressures are considered during the spudcan penetration into the soil. This is in line with standard design procedure of spudcans in sand (Jostad, H. P., et al., 2015). After the pre-driving load is applied, the operational load is held constant for a few seconds before the loading of the pile starts. During the first 8 seconds of the simulation, the self-weight of the pile is considered alongside the pre-driving and operational load of the spudcan. This phase is modeled under ideally drained conditions, as rapid pile penetration due to self-weight is typically avoided by the crane operator. Since no significant pile-spudcan interaction is expected during this phase, the self-weight penetration of the pile is simulated simultaneously with the spudcan penetration.

After the first 8 seconds, the loading of the pile by the mass of the hammer is modeled as a linearly increasing load on the pile head, while impact blows are simultaneously applied. The full external force history (not showing the self-weight of the pile) is provided in Figure 3. The hammer blows are applied at a frequency of 0.65 Hz with an impact duration of 20 ms, delivering approximately 400 kJ of energy per blow. This part of the simulation considers partially drained conditions, i.e. excess pore water pressures and consolidation effects.

A comparison of models using one versus two finite elements below the monopile tip reveals differences in predicted pile penetration depth as can be seen from Figure 4. Vertical displacements u_z normalized by the monopile diameter D_m are depicted in this plot. The displacements of both the pile and the spudcan are visualized, along with the external forces applied to the pile, which include the mass of the hammer and the impact blows.

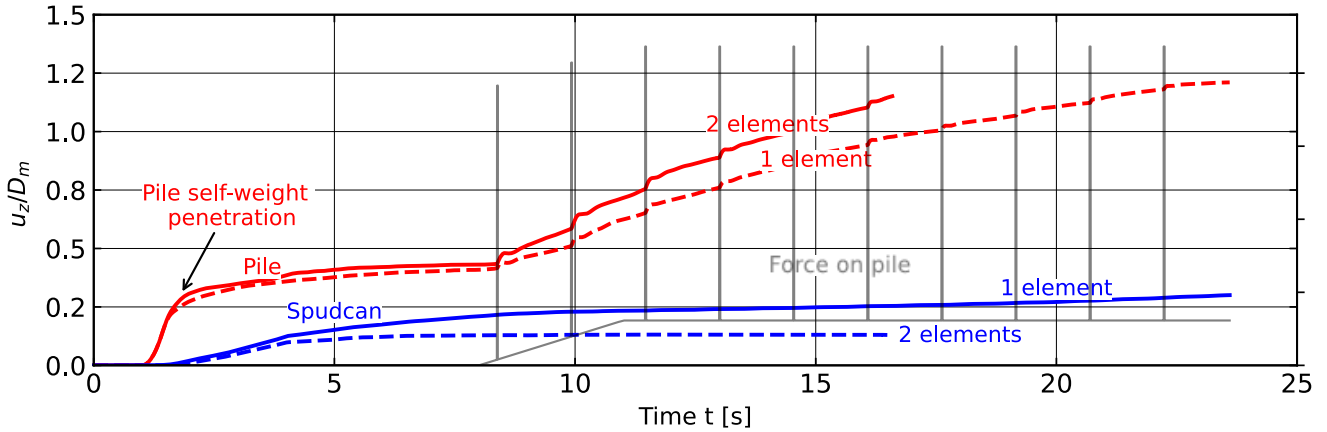


Figure 4. Vertical displacements u_z normalized by the monopile diameter D_m for the monopile and the spudcan for two different meshes with one or two elements below the pile tip

The self-weight penetration of the pile leads to approximately half the pile diameter in penetration depth. This depth increases slightly when two elements are used below the pile tip, aligning with previous studies showing reduced pile tip resistance and hence more penetration in response to the same applied loading for a finer mesh discretization. Notably, the spudcan is also affected by the number of elements below the pile tip, though to a lesser degree. This is mainly attributed to the reduced critical time increment due to the smaller element size in case of 2 elements below the pile tip rather than a stronger influence from the pile installation on the spudcan.

Once the external load on the pile is applied, the pile exhibits a higher penetration rate. Due to the model's complexity, only a limited number of impact blows could be simulated, as they result in very high computational times and with increasing pile penetration rapidly decreasing critical time increments, which govern the maximum time increment and hence the computational speed of the simulation, occur.

2.2 Influence of the time between pre-driving of the spudcan and driving of the pile

As discussed in Section 2.1, it is important to ensure that the spudcan is close to static equilibrium following the pre-driving and subsequent operational loading. Only in this case can reliable data be obtained regarding its response during the pile driving process. To achieve static equilibrium faster, viscous pressures are considered to act on the spudcan, damping the oscillations that occur during the accelerated penetration process. Figure 4 compares the pile and spudcan response for different durations of the operational load phase. For the dashed line, the force-time history as depicted in Figure 3 is considered, whereas for the solid line, the operational load is six seconds longer. It is evident from Figure 4 that the duration of the operational load only slightly influences the spudcan behaviour during pile driving. Essentially, the spudcan reaches static equilibrium in both cases, meaning that the operational loading can be applied in only five seconds, as shown in Figure 3.

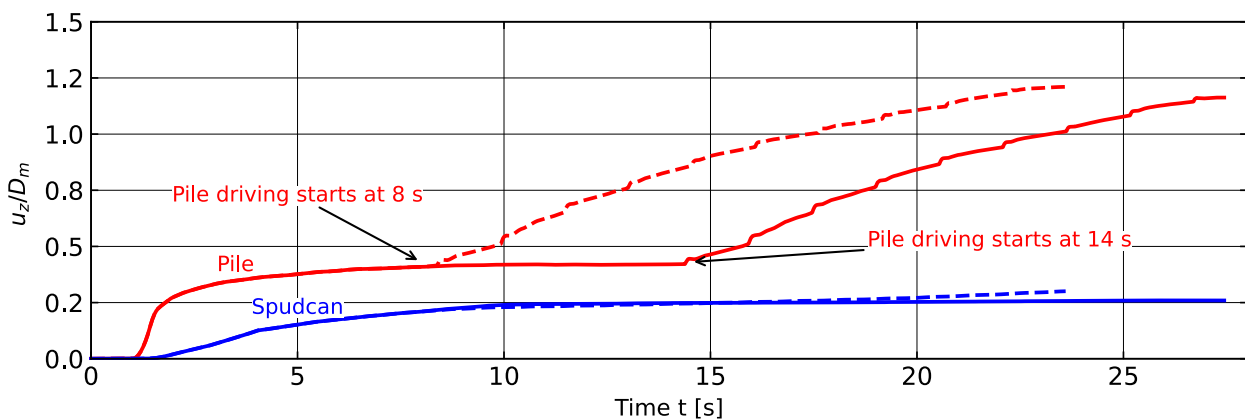


Figure 4. Vertical displacements u_z normalized by the monopile diameter D_m for the monopile and the spudcan for different durations of the operational load of the spudcan, i.e. different times at which the pile driving starts

2.3 Spudcan behaviour during monopile or jacket-pile installation

Vertical displacements u_z of the spudcan are plotted for different scenarios in Figure 5. These scenarios include simulations of monopile and jacket-pile installations in Karlsruhe Fine Sand (KFS), including a case without driving force in case of the jacket-pile. Because the spudcan only shows small oscillations, the installation of the monopile is judged not to influence the spudcan during driving, indicating minimal interaction effects in these configurations.

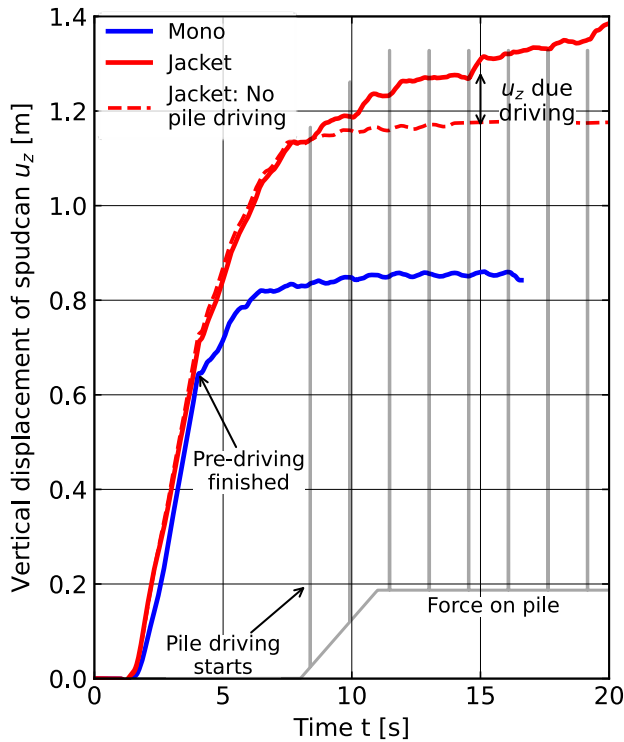


Figure 5. Vertical displacements of the spudcan considering monopile or jacket-pile installation. In the latter case, an additional simulation without driving force on the pile is shown with a dashed line.

In the case of jacket-piles, the spudcan exhibits considerable displacements during driving, indicating an interaction effect between the two structures. This suggests that the proximity and configuration of the jacket-pile relative to the spudcan lead to significant mutual influence.

Figure 6 shows the excess pore water pressure and effective horizontal stress (compression negative) for the most critical conditions being the jacket-pile installation. The configuration at the end of the simulation at approximately 20 s is depicted. It is visible that below both the spudcan and the pile considerable excess pore water pressures are present, while the distribution of effective stresses indicates interaction effects between spudcan and pile.

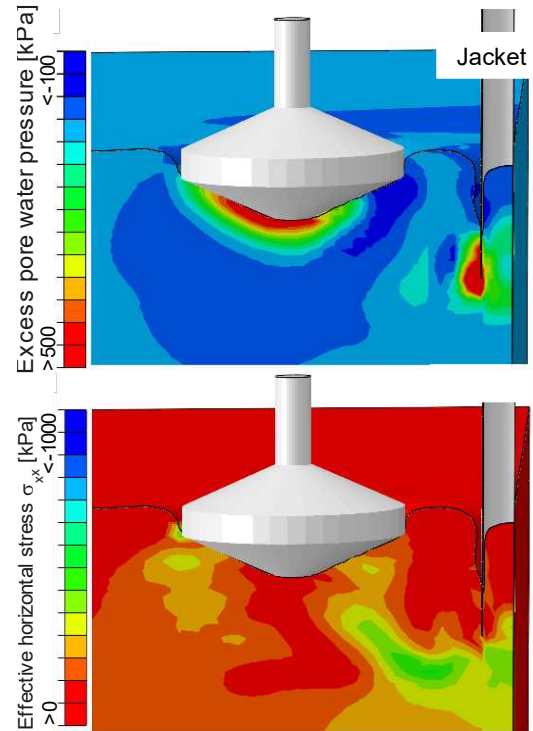


Figure 6. Excess pore water pressure and effective horizontal stress (compression negative) during the jacket-pile installation

3 DISCUSSION AND CONCLUSIONS

This paper presents the first numerical approach to study the interaction between spudcans and piles during installation, considering hydro-mechanically coupled effects, large deformations, and wave propagation. An attempt has been made to model the entire process of spudcan penetration as well as pile installation starting from the seabed. Given these aims, several challenges of the numerical modelling approach have been identified. Some of these challenges could be overcome, while others remain to be solved. The following list outlines these challenges, solutions and suggests potential improvements for future analyses.

First, the entire process is modelled dynamically, potentially alongside consolidation, in physical time. Since the size of time increments is limited in dynamic analyses, the physical time modelled had to be accelerated. This led to the pile's self-weight penetration occurring simultaneously with the spudcan's penetration into the soil. This decision was made under the assumption that the relatively slow self-weight penetration of the pile would not significantly affect the spudcan's behaviour during its installation. This simulation phase was performed under fully drained conditions.

Second, because all simulation steps are performed dynamically, the spudcan might not be in static equilibrium when the pile installation process begins.

This non-equilibrium condition could cause the spudcan to accumulate settlement, even in the absence of pile installation. This challenge could be effectively addressed by considering viscous pressure on the spudcan, allowing to reach static equilibrium even in a short physical time during the dynamic steps of spudcan penetration during pre-driving and operational load. It was demonstrated that the spudcan shows only slight movement prior to the pile installation process following this approach.

Finally, the forces on the pile, including hammer blows and the self-weight of the driving equipment, were applied in a short physical time. In this process, partially drained conditions were considered. This may influence the results, as consolidation processes would typically play a more important role over a longer timeframe.

Another limitation of the current work is the assumption of a rigid pile, not considering the shock waves travelling in the pile during driving. Future work will investigate how this assumption influences the results using the recently proposed IMEX approach (Staubach & Macháček, 2024).

Despite these limitations, the following findings can be observed from the simulations: The installation of large 6.5 m diameter monopiles at 21 m from the spudcan does not lead to notable displacements of the spudcan as shown in Figure 5. In contrast, the installation of smaller jacket-piles located closer to the spudcan may lead to interaction effects between the spudcan and pile, negatively impacting the spudcan and resulting in settlements. This model shows interaction is possible between pile and spudcan. Further work is required to validate the numerical results by centrifuge or field tests.

AUTHOR CONTRIBUTION STATEMENT

Patrick Staubach: Software, Data curation, Formal Analysis, Supervision, Visualization, Conceptualization, Methodology, Writing-Original draft. **Marie Lücke:** Software, Data curation, Visualization, Formal Analysis. **Sylvie Raymackers:** Conceptualization, Writing- Reviewing and Editing. **Britta Bienen:** Formal Analysis, Supervision, Conceptualization, Methodology, Writing- Reviewing and Editing.

REFERENCES

- Chow, Y.K., Kencana, E.Y., Leung, C.F. and Purwana, O.A. (2021). Spudcan-pile interaction in thick soft clay and soft clay overlying sand: A simplified numerical solution, *Appl Ocean Res*, 112, 102684
- Niemunis, A., & Herle, I. (1997). Hypoplastic model for cohesionless soils with elastic strain range. *Mech Cohesive-Frict Mater*, 2(4), 279–299.
- Falcon, S. D., Choo, Y. W., and Leung, C. F. (2023). Spudcan–pile interaction in sand-over-clay: centrifuge modelling. *Géotechnique*, 73(6), 480–494.
- Hamann, T., Qiu, G., and Grabe, J. (2015). Application of a coupled eulerian–lagrangian approach on pile installation problems under partially drained conditions. *Comp. and Geotechnics*, 63, 279–290.
- Jostad, H. P., et al. (2015). Guidelines for the site-specific geotechnical analyses of jack-ups. Norwegian Petroleum Directorate.
- Staubach, P., Macháček, J., Moscoso, M. C., and Wichtmann, T. (2020). Impact of the installation on the long-term cyclic behaviour of piles in sand: a numerical study. *Soil Dyn Earthq Eng* 138, 106223.
- Staubach, P., Macháček, J., Bienen, B. and Wichtmann, T. (2022). Long-term response of piles to cyclic lateral loading following vibratory and impact driving in water-saturated sand, *J. Geotech. Geoenv. Eng* 148(11):4022097.
- Staubach, P., Tschirschky, L., Macháček, J. and Wichtmann, T. (2023). Monopile installation in clay and subsequent response to millions of lateral load cycles. *Comp. and Geotechnics*, 155, 105221
- Staubach, P., Macháček, J. (2024). Spatially mixed implicit-explicit schemes in hydro-mechanically coupled soil dynamics. *Comp. and Geotechnics*, 176, 106811.
- Staubach, P. (2024). Hydro-mechanically coupled CEL analyses with effective contact stresses. *Int J Numer Anal Methods Geomech*, 48, 2207–2215.
- Tho, K.K., Leung, C.F., Chow, Y.K. and Swaddiwudhipong, S. (2013). Eulerian finite element simulation of spudcan–pile interaction. *Can. Geo. J.* 50 (6), 595–608.
- von Wolffersdorff, P. (1996). A hypoplastic relation for granular materials with a predefined limit state surface. *Mechanics of Cohesive-frictional Materials*, 1(3), 251–271.
- Wang, D., Bienen, B., Nazem, M., Tian, Y., Zheng, J., Pucker, T., and Randolph, M. F. (2015). Large deformation finite element analyses in geotechnical engineering. *Comp. and Geotechnics*, 65, 104–114.
- Wichtmann, T. (2016). Soil behaviour under cyclic loading - experimental observations, constitutive description and applications. Habilitation thesis, Publications of the Institute of Soil Mechanics and Rock Mechanics, KIT, Issue No. 181.
- Wu, H., Atangana Njock, P. G., Chen, J., and Shen, S. (2019). Numerical simulation of spudcan-soil interaction using an improved smoothed particle hydrodynamics method. *Mar Struct* 66, 213–226.

INTERNATIONAL SOCIETY FOR SOIL MECHANICS AND GEOTECHNICAL ENGINEERING



This paper was downloaded from the Online Library of the International Society for Soil Mechanics and Geotechnical Engineering (ISSMGE). The library is available here:

<https://www.issmge.org/publications/online-library>

This is an open-access database that archives thousands of papers published under the Auspices of the ISSMGE and maintained by the Innovation and Development Committee of ISSMGE.

The paper was published in the proceedings of the 5th International Symposium on Frontiers in Offshore Geotechnics (ISFOG2025) and was edited by Christelle Abadie, Zheng Li, Matthieu Blanc and Luc Thorel. The conference was held from June 9th to June 13th 2025 in Nantes, France.